Two Photon Fluorescence Microscopy of Coexisting Lipid Domains in Giant Unilamellar Vesicles of Binary Phospholipid Mixtures

L. A. Bagatolli and E. Gratton
Laboratory for Fluorescence Dynamics, University of Illinois at Urbana-Champaign, Urbana, Illinois 61801 USA

ABSTRACT Images of giant unilamellar vesicles (GUVs) formed by different phospholipid mixtures (1,2-dipalmitoyl-*sn*-glycero-3-phosphocholine/1,2-dilauroyl-*sn*-glycero-3-phosphocholine (DPPC/DLPC) 1:1 (mol/mol), and 1,2-dipalmitoyl-*sn*-glycero-3-phosphoethanolamine/1,2-dipalmitoyl-*sn*-glycero-3-phosphocholine (DPPE/DPPC), 7:3 and 3:7 (mol/mol) at different temperatures were obtained by exploiting the sectioning capability of a two-photon excitation fluorescence microscope. 6-Dodecanoyl-2-dimethylamino-naphthalene (LAURDAN), 6-propionyl-2-dimethylamino-naphthalene (PRODAN), and Lissamine rhodamine B 1,2-dihexadecanoyl-*sn*-glycero-3-phosphoethanolamine (*N*-Rh-DPPE) were used as fluorescent probes to reveal domain coexistence in the GUVs. We report the first characterization of the morphology of lipid domains in unsupported lipid bilayers. From the LAURDAN intensity images the excitation generalized polarization function (GP) was calculated at different temperatures to characterize the phase state of the lipid domain. On the basis of the phase diagram of each lipid mixture, we found a homogeneous fluorescence distribution in the GUV images at temperatures corresponding to the fluid region in all lipid mixtures. At temperatures corresponding to the phase coexistence region we observed lipid domains of different sizes and shapes, depending on the lipid sample composition. In the case of GUVs formed by DPPE/DPPC mixture, the gel DPPE domains present different shapes, such as hexagonal, rhombic, six-cornered star, dumbbell, or dendritic. At the phase coexistence region, the gel DPPE domains are moving and growing as the temperature decreases. Separated domains remain in the GUVs at temperatures corresponding to the solid region, showing solid-solid immiscibility. A different morphology was found in GUVs composed of DLPC/DPPC 1:1 (mol/mol) mixtures. At temperatures corresponding to the phase coexistence, we observed the gel domains as line defects in the GUV surface. These lines move and become thicker as the temperature decreases. As judged by the LAURDAN GP histogram, we concluded that the lipid phase characteristics at the phase coexistence region are different between the DPPE/DPPC and DLPC/DPPC mixtures. In the DPPE/DPPC mixture the coexistence is between pure gel and pure liquid domains, while in the DLPC/DPPC 1:1 (mol/mol) mixture we observed a strong influence of one phase on the other. In all cases the domains span the inner and outer leaflets of the membrane, suggesting a strong coupling between the inner and outer monolayers of the lipid membrane. This observation is also novel for unsupported lipid bilayers.

INTRODUCTION

Biological membranes are multimolecular bidimensional arrangements composed mainly of proteins and lipids. Although cells contain many different types of lipids, phospholipids are the major components of biological membranes. In particular, phosphatidylcholines and phosphatidylethanolamines are the two major components in eukaryotic cell membranes (Hauser and Poupart, 1992). How do the physical properties of lipid molecules influence the structure and function of cell membranes? Studies of the physicochemical properties of artificial lipid systems, where the lipid composition and environmental conditions (such as temperature, ionic strength, pH, etc.) can be systematically controlled, provide information about the behavior of the lipid matrix. In particular, understanding phase equilibria in two-component lipid bilayers constitutes a necessary step in the description of multicomponent lipid systems. One important source of information about the phase equilibria of lipid mixtures is the phase diagram. In the last 25 years, phase diagrams for different two-component phospholipid mixtures have been constructed using both theoretical and experimental approaches. Theoretical calculations were made, using computers models to build the phospholipid phase diagrams (Ipsen and Mouritsen, 1988; Jørgensen and Mouritsen, 1995). Furthermore, an array of experimental techniques such as differential scanning calorimetry, fluorescence spectroscopy, NMR, x-ray diffraction, and electron spin resonance have been used to construct lipid phase diagrams of binary mixtures (Lee, 1975; Lentz et al., 1976; Mabrey and Sturtevant, 1976; Van Dijck et al., 1977; Arnold et al., 1981; Blume et al., 1982; Caffrey and Hing, 1987; Shimshick and McConnell, 1973). An interesting region in lipid phase diagrams is that corresponding to the coexistence of the fluid and solid phase. Phase separation arises in general only if one of the components is in the gel state (Sackmann, 1994). One interesting aspect of phase separation in vesicles is the formation of a stable domain structure discovered in 1977 (Gebhardt et al., 1977). Phase separation plays a central role in the stabilization of multicomponent vesicles in fluid-solid coexistence and in the fission of small vesicles after budding (Sackmann and Feder, 1995). The lipid domains in vesicles at the phase

Received for publication 21 June 1999 and in final form 14 September 1999.

Address reprint requests to Dr. Luis A. Bagatolli, Laboratory for Fluorescence Dynamics, 184 Loomis Lab., 1110 West Green St., Urbana, IL 61801. Tel.: 217-244-5620; Fax: 217-244-7187; E-mail: lab@alecto.physics.uiuc.edu.

0006-3495/00/01/290/16 $2.00

coexistence region were visualized directly by electron microscopy (Sackmann, 1978). However, there is a dearth of experimental approaches that allow direct visualization of lipid domains (shape and dynamics) in lipid vesicles under the same experimental conditions as in classical approaches (such as differential scanning calorimetry, fluorescence spectroscopy, etc.).

The characteristics of the lipid samples, such as size, lamellarity, radius of curvature, and shape, are strongly dependent on the method used to form the vesicles (Lasic, 1988). As a consequence of the preparation method, the parameters that characterize the lipid phase equilibrium in lipid mixtures are affected by the lipid sample characteristics. Because the size of the giant unilamellar vesicles (GUVs) is on the same order as the size of cells, and single vesicles can be directly observed under the microscope, GUVs are becoming objects of intense scrutiny in diverse areas that focus on membrane behavior (Menger and Keiper, 1998). The mechanical properties of model membranes have been intensely studied using GUVs (Evans and Kwok, 1982; Needham et al. 1988; Needham and Evans 1988; Meléard et al., 1997, 1998; for reviews see Sackmann, 1994; Menger and Keiper, 1998). These studies revealed the physical properties of the membranes through the calculation of elementary deformation parameters. A similar study using the same temperature range and experimental approach was reported for GUVs composed of mixtures of phosphatidylcholine phospholipids and cholesterol (Needham et al., 1988). In a previous work we reported shape hysteresis in single-component GUVs at the phase transition temperature (Bagatolli and Gratton, 1999). Our approach was based on the sectioning effect of the two-photon fluorescence microscope and the well-characterized fluorescent properties of 6-dodecanoyl-2-dimethylamine-naphthalene (LAURDAN) (Bagatolli and Gratton, 1999). LAURDAN′s fluorescence parameters are sensitive to changes in the water content in the lipid bilayers and, as a consequence, to the lipid phase state (see review articles on LAURDAN properties by Parasassi and Gratton, 1995; Parasassi et al., 1997, 1998; Bagatolli et al., 1997, 1998). In this work we present an extended application of our experimental approach (Bagatolli and Gratton, 1999), including two other fluorescent probes, namely Lissamine rhodamine B 1,2-dihexadecanoyl-*sn*-glycero-3-phosphoethanolamine (*N*-Rh-DPPE) and 6-propionyl-2-dimethylamino-naphthalene (PRODAN). Our strategy is based on monitoring single GUVs composed of 1,2-dipalmitoyl-*sn*-glycero-3-phosphoethanolamine /1,2-dipalmitoyl-*sn*-glycero-3-phosphocholine (DPPE/DPPC) or 1,2-dilauroyl-*sn*-glycero-3-phosphocholine/1,2-dipalmitoyl-*sn*-glycero-3-phosphocholine (DLPC/DPPC) mixtures at different temperatures. We show novel microscopic pictures of the vesicle lateral organization at different temperature regimes of the corresponding phase diagram. The unique properties of unsupported GUVs allow us to make new observations of the shape and morphology of lipid domains in an environment similar to that found in cells.

MATERIALS AND METHODS

Materials

LAURDAN, PRODAN, and *N*-Rh-DPPE were from Molecular Probes (Eugene, OR). 1-Palmitoyl, 2-oleoyl-*sn*-glycero-3-phosphocholine (POPC), DLPC, DPPC, and DPPE were from Avanti Polar Lipids (Alabaster, AL) and were used without further purification.

Methods

Vesicle preparation

Stock solutions of phospholipids were made in chloroform. The concentration of the lipid stock solutions was 0.2 mg/ml. For GUV preparation we followed the electroformation method developed by Angelova and Dimitrov (Angelova and Dimitrov, 1986; Dimitrov and Angelova, 1987; Angelova et al., 1992). To grow the GUVs, a special temperature-controlled chamber, which was previously described (Bagatolli and Gratton, 1999), was used. The experiments were carried out in the same chamber after the vesicle formation, using an inverted microscope (Axiovert 35; Zeiss, Thornwood, NY). The following steps were used to prepare the GUVs: 1) ~3 μl of the lipid stocks solution was spread on each Pt wire under a stream of N_2. To remove the residues of organic solvent the samples were lyophilized for ~2 h. 2) To add the aqueous solvent inside the chamber (Millipore water 17.5 MΩ/cm), the bottom part of the chamber was sealed with a coverslip. The water was previously heated to the desired temperature (above the lipid mixture phase transition, 70°C for DPPE/DPPC 7:3 and 3:7 (mol/mol) mixtures and 50°C for DLPC/DPPC and POPC/DPPC 1:1 (mol/mol) mixtures), and then sufficient water was added to cover the Pt wires. Just after this step the Pt wires were connected to a function generator (Hewlett-Packard, Santa Clara, CA), and a low-frequency AC field (sinusoidal wave function with a frequency of 10 Hz and an amplitude of 3 V) was applied for 90 min. After the vesicle formation, the AC field was turned off and the temperature scan (from high to low temperatures) was initiated. The GUV yield was ~95%, and the mean diameter of the GUVs was ~30 μm. A CCD color video camera (CCD-Iris; Sony) in the microscope was used to follow vesicle formation and to select the target vesicle. The temperature was measured inside the sample chamber with a digital thermocouple (model 400B; Omega, Stamford, CT) with a precision of 0.1°C. The LAURDAN labeling procedure was done in one of two ways. Either the fluorescent probe was premixed with the lipids in chloroform, or a small amount (less than 1 μl) of LAURDAN in dimethyl sulfoxide (DMSO) was added after the vesicle formation (final LAURDAN/lipid ratio 1:500 (mol/mol) in both cases). The sample behavior during the temperature scan was independent of the labeling procedure. PRODAN labeling was carried out by the addition of PRODAN in DMSO (less than 1 μl of DMSO stock solution; final PRODAN/lipid ratio 1:500, mol/mol). In the case of *N*-Rh-DPPE the lipid was premixed with the fluorescent phospholipid in chloroform. The percentage of *N*-Rh-DPPE in the sample was less than 0.5 mol%. To check the lamellarity of the giant vesicles we imaged several vesicles (up to 20 vesicles in different regions of the Pt wires) labeled with LAURDAN or *N*-Rh-DPPE, using the two-photon excitation microscope. We found that the intensities measured in the border of different vesicles in the liquid crystalline phase were very similar. Because the existence of multilamelar vesicles would give rise to different intensity images due to the presence of different numbers of LAURDAN labeled lipid bilayers, we concluded that the vesicles were unilamellar, in agreement with previous observations in GUVs with the electroformation method (Mathivet et al., 1996).

Two-photon fluorescent measurements

GP function

LAURDAN′s emission spectrum is blue in the lipid gel phase, while in the liquid crystalline phase it moves during the excited-state lifetime from the blue to the green (Parasassi et al. 1990, 1991). To quantify the emission spectral changes, the excitation generalized polarization (GP) function was defined analogously to the fluorescence polarization function as

$$GP = \frac{I_B - I_R}{I_B + I_R}$$

where I_B and I_R correspond to the intensities at the blue and red edges of the emission spectrum (respectively) for a given excitation wavelength (Parasassi et al., 1990, 1991).

Experimental apparatus for two-photon excitation microscopy measurements

Two-photon excitation is a nonlinear process in which a fluorophore absorbs two photons simultaneously. Each photon provides half the energy required for excitation. The high photon densities required for two-photon absorption are achieved by focusing a high peak power laser light source on a diffraction-limited spot through a high numerical aperture objective. Therefore, in the areas above and below the focal plane, two-photon absorption does not occur, because of insufficient photon flux. This phenomenon allows a sectioning effect without the use of emission pinholes, as in confocal microscopy. Another advantage of two-photon excitation is the low extent of photobleaching and photodamage above and below the focal plane. For our experiments we used a scanning two-photon fluorescence microscope developed in our laboratory (So et al., 1995, 1996). For the LAURDAN GP measurements we used a procedure similar to that previously described (Yu et al., 1996; Parasassi et al., 1997, Bagatolli and Gratton, 1999). We used a LD-Achroplan 20× long working distance air objective (Zeiss, Homldale, NJ) with a N.A. of 0.4. A titanium-sapphire laser (Mira 900; Coherent, Palo Alto, CA) pumped by a frequency-doubled Nd:vanadate laser (Verdi; Coherent) was used as the excitation light source. The excitation wavelength was set at 780 nm. The laser was guided by a galvanometer-driven *x-y* scanner (Cambridge Technology, Watertown, MA) to achieve beam scanning in both the *x* and *y* directions. The scanning rate was controlled by the input signal from a frequency synthesizer (Hewlett-Packard, Santa Clara, CA), and a frame rate of 25 s was used to acquire the images (256 × 256 pixels). The laser power was attenuated to 50 mW before the light entered the microscope through a polarizer. The samples received about one-tenth of the incident power. To change the polarization of the laser light from linear to circular, a quarter wave plate (CVI Laser Corporation, Albuquerque, NM) was placed after the polarizer. The fluorescence emission was observed through a broad band-pass filter from 350 nm to 600 nm (BG39 filter; Chroma Technology, Brattleboro, VT). For the case of LAURDAN GP calculations, two additional optical band-pass filters with 46 nm width and centered at 446 nm and at 499 nm (Ealing electro-optics, New Englander Industrial Park, Holliston, MA) were used to collect fluorescence in the blue and green regions of LAURDAN′s emission spectrum, respectively. A miniature photomultiplier (R5600-P; Hamamatsu, Brigdewater, NJ) was used for light detection in the photon counting mode. A home-built card in a personal computer acquired the counts.

Vesicle image measurements

We obtained the images of the GUVs in the chamber, using the Pt wires as a "holder." The vesicles were attached to the Pt wires, which were covered by a lipid film. The diameters of the vesicles were measured by using size-calibrated fluorescent spheres. We determined that the pixel size in our experiments corresponds to 0.52 μm.

In a previous study, Parasassi et al. showed that polarized light excitation of LAURDAN-labeled multilamellar vesicles caused a photoselection effect in the fluorescence emission image (Parasassi et al., 1997). This effect was recently confirmed in GUVs composed of pure phospholipid (Bagatolli and Gratton, 1999). The electronic transition dipole of LAURDAN in lipid vesicles is aligned parallel to the hydrophobic lipid chains (see Fig. 1) (Parasassi and Gratton, 1995; Parasassi et al., 1998). Consider the linear polarization confined in the *x-y* plane. By exploring different regions of a spherical vesicle (at a given vertical section) we can observe that the strong excitation occurs in the direction parallel to the excitation polarization, whereas poor excitation will occur in regions perpendicular to the excitation polarization (Fig. 1 *a*; Parasassi et al., 1997; Bagatolli and Gratton, 1999). In particular, this effect will be stronger in the *x-y* plane that passes through the center of the sphere. If we observe the top or bottom regions of a spherical lipid vesicle we will find poor excitation. In addition, this effect depends on the phase state of the phospholipids. In the gel phase the packing of the lipid molecules is very tight, increasing the photoselection effect (Fig. 1 *a*; Parasassi et al., 1997; Bagatolli and Gratton, 1999). In the fluid phase we expect to have a component of the transition dipole of LAURDAN parallel to the excitation polarization because of the relatively low lipid order. As a consequence of the reduced order, there is less difference in the emission intensity between the parallel and perpendicular orientations of LAURDAN′s electronic transition dipole (Fig. 1 *a*; Parasassi et al., 1997; Bagatolli and Gratton, 1999). An important observation is that polarized light, which photoselects well-oriented LAURDAN molecules, also selects LAURDAN molecules associated with high GP values (Parasassi et al., 1997; Bagatolli and Gratton, 1999). With polarized excitation, if the image contains separate domains (pixels) of different GP values, the higher GP value domains appear parallel to the excitation polarization (see Fig. 1 *b*). This effect was used to ascertain lipid domain coexistence in multilamellar vesicles composed of DLPC/DPPC mixtures and GUVs composed of pure phospholipids (Parasassi et al., 1997; Bagatolli and Gratton, 1999). In Fig. 1 *b* we present a sketch of the three different situations considered by Parasassi et al., showing the relationship between the pixel and the lipid domain size (Parasassi et al., 1997):

1. *Lipid domains smaller than the pixel size*. We will have an average GP value per pixel in the image. Because we can photoselect the high GP domains, the GP image will show separation between the high and low GP regions, i.e., the high GP region will be aligned parallel to the excitation polarization orientation while the low GP region will be aligned perpendicular to the excitation polarization orientation.

2. *Lipid domains comparable to the pixel size*. In this case the high GP region will again be aligned parallel to the excitation polarization orientation. In the case of the low GP domains, they will present a homogeneous distribution around the vesicle contour.

3. *Lipid domains bigger than the pixel size*. Clearly separated GP regions should be observed.

RESULTS

GUVs formed by DPPE/DPPC mixtures

Fig. 2 shows the LAURDAN GP images and the respective GP histograms of GUVs composed of the DPPE/DPPC 7:3 (mol/mol) mixture at different temperatures (Fig. 2, *a* and *b*, respectively). These images represent an *x-y* plane passing through the center of the GUVs. Between 70°C and 58°C the LAURDAN GP histogram is broad and centered at low GP values (~ 0.0) (Fig. 2 *b*). Between 57°C and 42°C the LAURDAN GP images show two regions of different GP (Fig. 2 *a*). In this case, the LAURDAN GP histogram is

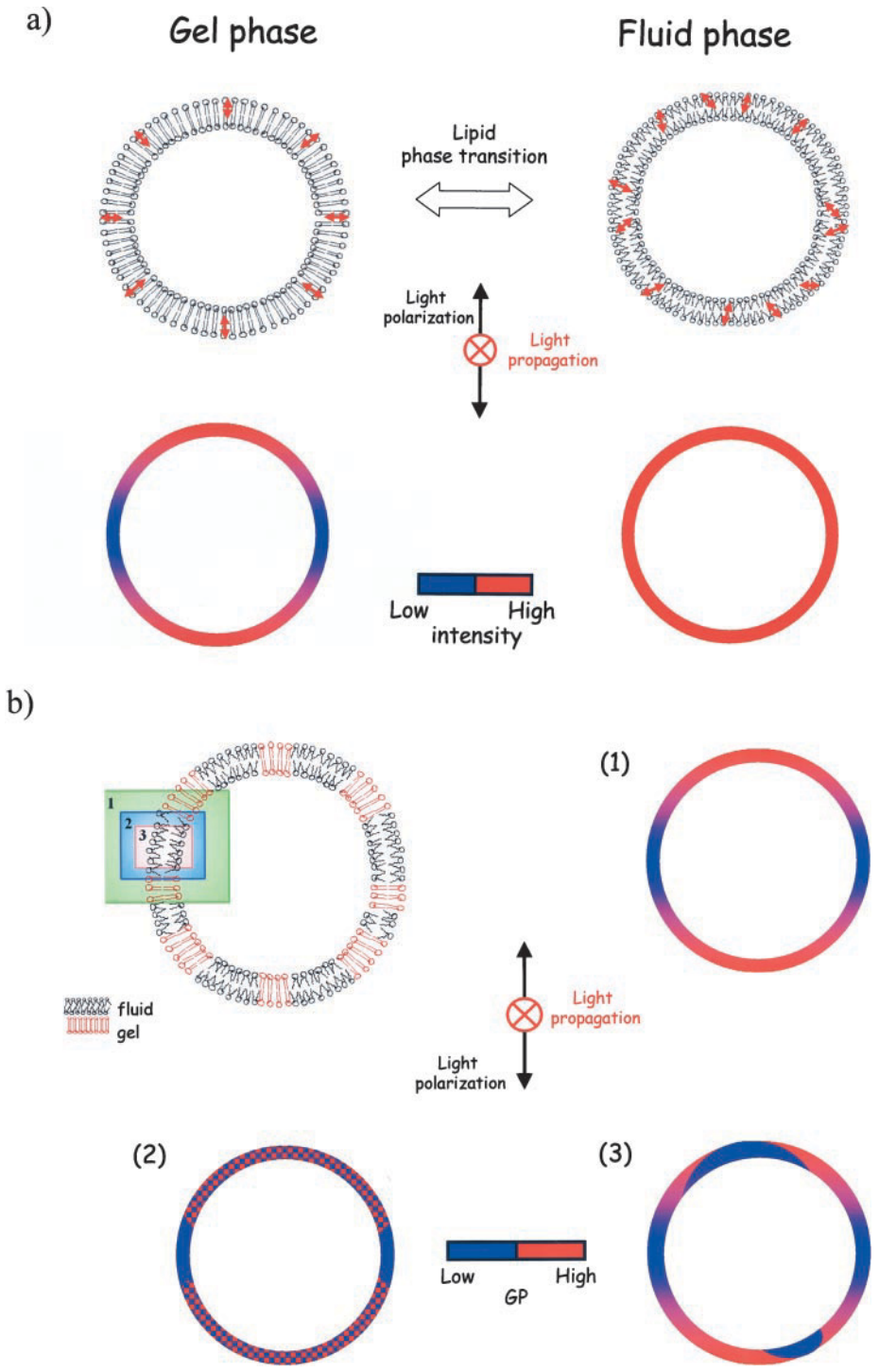

FIGURE 1 Schematic representation of the photoselection effect using LAURDAN in GUVs. (*A*) LAURDAN transition dipole (*red arrow*) orientation (*top*) and emission intensity pattern in a section of a single GUV (*bottom*) in the gel and fluid phases. (*B*) LAURDAN GP pattern in vesicles, assuming phase coexistence by effect of the photoselection (see text). (*1*) Lipid domains smaller than the pixel size; (*2*) lipid domains comparable to the pixel size; (*3*) lipid domains bigger than the pixel size.

bimodal, with center values of 0.12 and 0.51 for each histogram (Fig. 2 *b*). The center of the fluid and solid components of the GP histograms at the phase coexistence region are similar to those obtained in the fluid and solid temperature regions of the mixture (Fig. 2 *b*). The GP histogram centered at low GP values is broader than that centered at high GP values (Fig. 2 *b*). Below 42°C we found a LAURDAN GP histogram centered at high GP values (~0.56). The width of the LAURDAN GP histogram below 42°C is narrower than that found at temperatures above 58°C.

Using *N*-Rh-DPPE, the vesicles were imaged in the top or bottom region. Above 58°C in GUVs formed by DPPE/DPPC 7:3 (mol/mol) we observed a homogeneous distribution of the fluorescent molecules (Fig. 3). For GUVs formed with DPPE/DPPC 3:7 (mol/mol) we observed the same

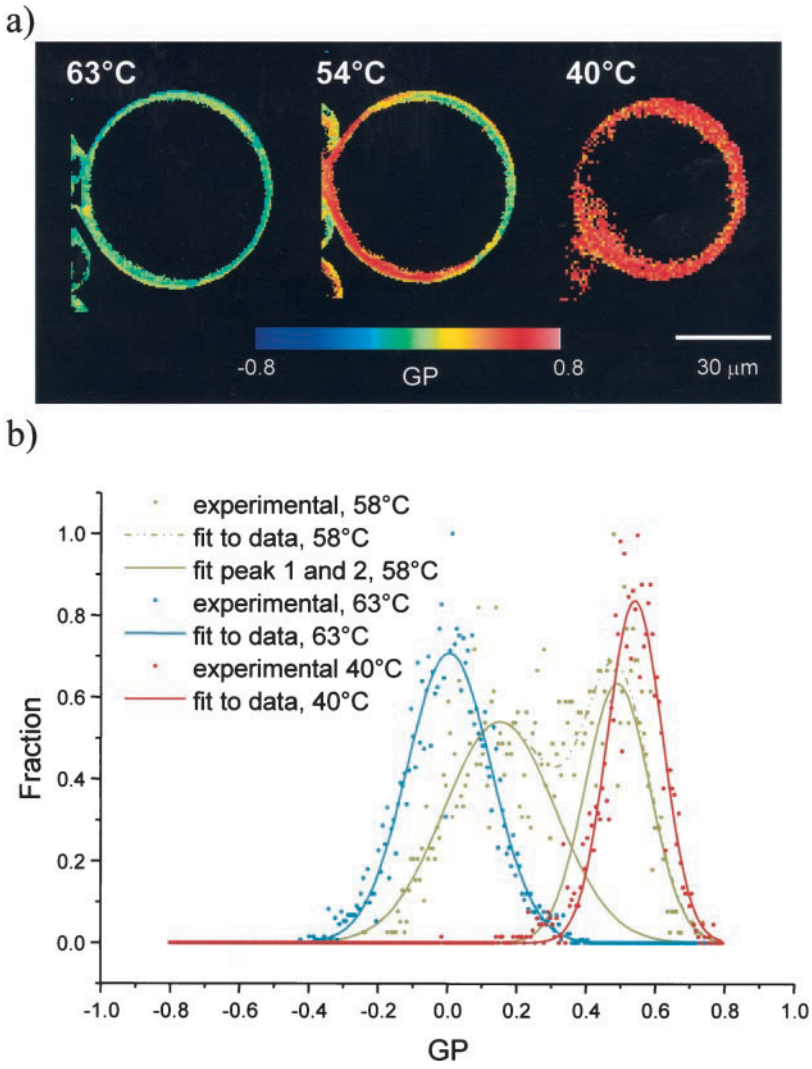

FIGURE 2 (*a*) Two-photon excitation LAURDAN GP images of a single GUV composed of DPPE/DPPC 7:3, obtained with circular polarization light. (*b*) Experimental and fitted GP histograms corresponding to the three images presented in *a*. For the fitting procedure we used Gaussian functions.

situation above 49°C (not shown). At 58°C and 48°C for GUVs composed of DPPE/DPPC 7:3 and 3:7, respectively, we observed nonfluorescent areas in the vesicle surface coexisting with fluorescent regions. These nonfluorescent regions move and grow as the temperature is decreased (Fig. 3). We note that such domain structures are not apparent in traditional light microscopy images (Fig. 4). The nonfluorescent domains in different vesicles and often on the same vesicle have a particular shape, namely hexagonal, rhombic, six-cornered star, dumbbell, and dendritic (see Fig. 5). Below 42°C for both GUVs formed by DPPE/DPPC 7:3 and 3:7 (mol/mol) the nonfluorescent areas were fixed in one position (Fig. 6). These nonfluorescent areas have quasicircular and dendritic shapes. The relative amount of nonfluorescent areas in GUVs formed by DPPE/DPPC 7:3 and 3:7 (mol/mol) mixtures is consistent with the DPPE molar fraction in the mixtures. Therefore we conclude that the nonfluorescent areas are formed by DPPE in the gel phase. In this particular mixture, the *N*-Rh-DPPE molecules are segregated from the gel DPPE domains and locate in the DPPC liquid crystalline domains of the vesicle.

To verify that the nonfluorescent areas in the GUVs correspond to DPPE gel domains, we used PRODAN as a fluorescent probe. PRODAN has a partition into the fluid phase, which is 35 times larger than that for the gel phase (Zeng and Chong, 1995; Krasnowska et al., 1998). Above 58°C, in GUVs composed of DPPE/DPPC 7:3 (mol/mol) label with PRODAN, the fluorescence intensity in the GUV surface is homogeneously distributed (data not shown), as was observed with *N*-Rh-DPPE. Starting at 58°C, the GUV surface shows nonfluorescent areas coexisting with fluorescent areas, in agreement with those observed in GUVs formed by the same mixture and labeled with *N*-Rh-DPPE (Fig. 7). Taking into account the difference in PRODAN′s partition in the different lipid phases, we conclude that the nonfluorescent areas corresponded to DPPE gel domains. A similar picture was obtained using LAURDAN in DPPE/DPPC 7:3 (mol/mol) at the top or the bottom of the vesicles

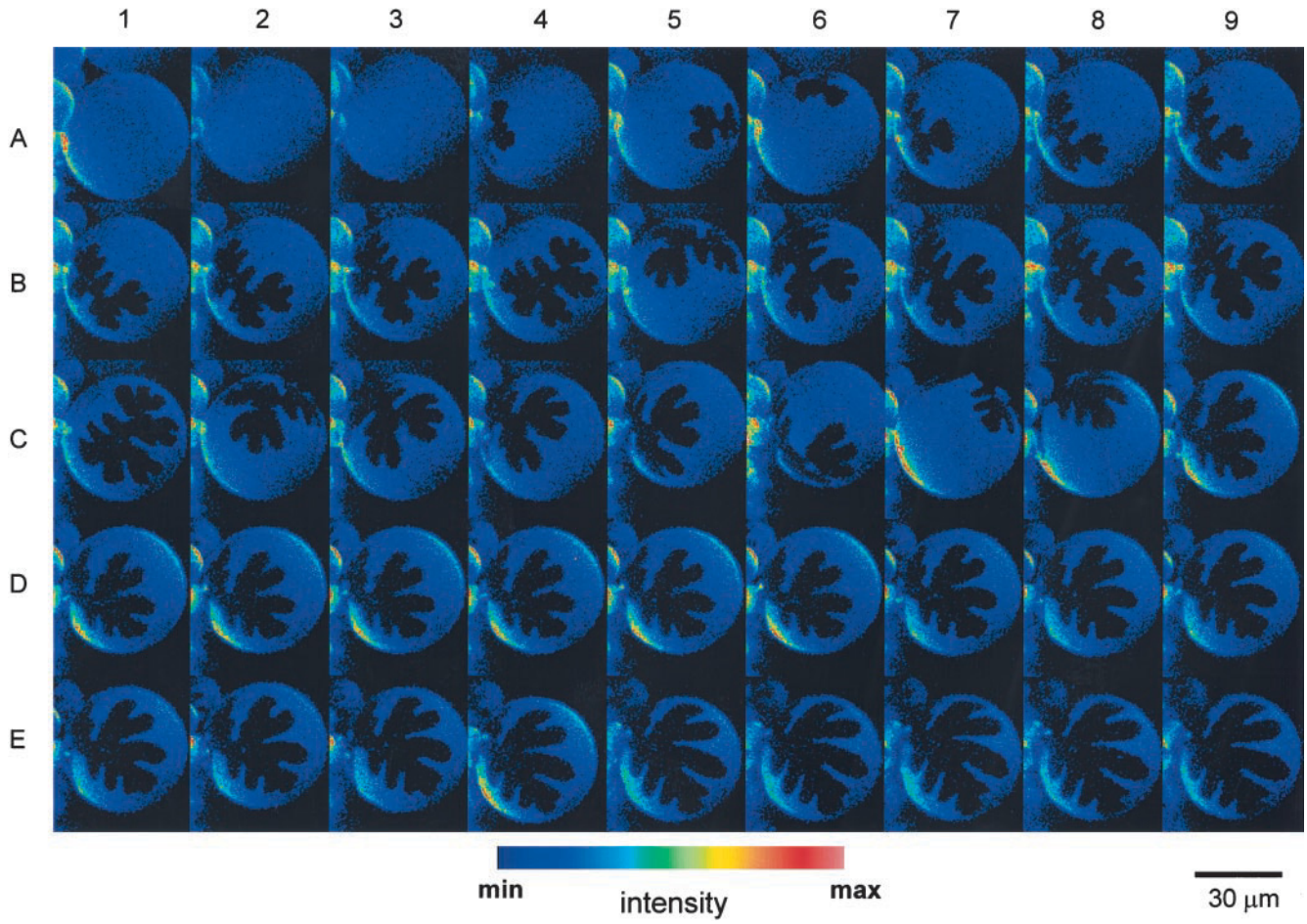

FIGURE 3 Two-photon excitation fluorescence intensity images of *N*-Rh-DPPE labeled GUVs formed by DPPE/DPPC 7:3 (mol/mol) (false color representation) as a function of temperature. The images have been taken at the top part of the GUV. The temperatures were as follows: *A1*, 65°C; *A2*, 62°C; *A3*, 59°C; *A4*, 56°C; *A5*, 55°C; *A6*, 54.8°C; *A7*, 54.7°C; *A8*, 54.5°C; *A9*, 54.2°C; *B1*, 54.1°C; *B2*, 53.9°C; *B3*, 53.8°C; *B4*, 53.7°C; *B5* and *B6*, 53.6°C; *B7* and *B8*, 53.4°C; *B9* and *C1*, 53.3°C; *C2* to *C4*, 53.2°C; *C5* to *C7*, 53.1°C; *C8* to *D5*, 53.0°C; *D6* to *E1*, 52.8°C; *E2*, 51.7°C; *E3*, 49.1°C; *E4*, 48.0°C; *E5*, 46.4°C; *E6*, 44.0°C; *E7*, 43.3°C; *E8*, 42.1°C; *E9*, 41.3°C.

(Fig. 7). LAURDAN is homogeneously distributed between the gel and liquid crystalline regions in the GUVs (compare Fig. 2 with Fig. 7). However, because the excitation light is polarized in the *x-y* plane and the LAURDAN dipole is well oriented along the membrane in the gel phase, i.e., in the *z* direction at the bottom or top of the vesicles (see Materials and Methods), we were not able to excite the gel domains in these regions of the GUV.

A novel feature connected to the lipid domain characteristic was observed. In GUVs composed of DPPE/DPPC mixtures and at temperatures corresponding to phase coexistence, the nonfluorescent areas in the GUV span both monolayers of the lipid membrane (Fig. 3).

GUVs formed by DLPC/DPPC 1:1 mixture

Fig. 8 shows the behavior of DLPC/DPPC 1:1 mixture with temperature. In this figure we compare GUVs labeled with LAURDAN, PRODAN, and *N*-Rh-DPPE. At temperatures above 36°C we observed a homogeneous distribution of the fluorescent molecules independently of the fluorescent molecule used. Below 36°C lines appear on the vesicle. These lines move around the surface of the GUV and the thickness of these lines increases as the temperature decreases (see Fig. 8). The partitioning of *N*-Rh-DPPE between the gel and the liquid crystalline phases in the DLPC/DPPC mixture is different from that found in the DPPE/DPPC mixture. The fluorescence intensity coming from the lines is higher than that coming from the rest of the surface (Fig. 8). We did not observe nonfluorescent areas in the GUV surface with *N*-Rh-DPPE. A similar picture was obtained in a POPC/DPPC 1:1 (mol/mol) mixture with *N*-Rh-DPPE (data not shown).

We also observed different fluorescence intensities between the lines and the rest of the GUV surface with PRODAN. In this case the low fluorescence intensity corresponds to the lines (Fig. 8). Therefore we conclude that the lines are more gel-like than the rest of the surface. We confirmed this conclusion by using LAURDAN as a fluo-

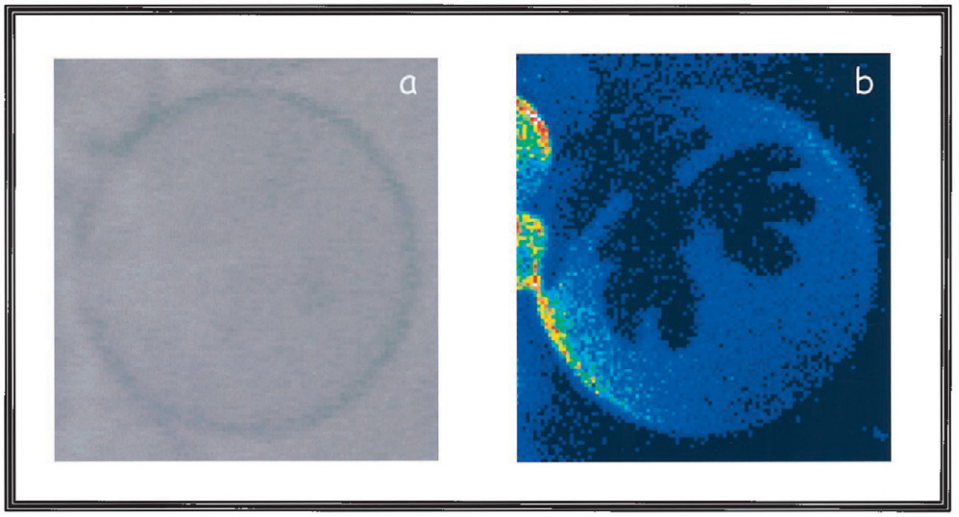

FIGURE 4 Light (*a*) and two-photon fluorescence (*b*) microscopy images of a single GUV described in Fig. 3, at 53.2°C.

rescent probe in the DPPC/DLPC GUVs. The GUV surface in this case shows nonfluorescent lines, supporting the hypothesis that the lines have a gel-like phase characteristic (Fig. 8). As in the DPPE/DPPC mixture, LAURDAN is homogeneously distributed between the phases (compare Figs. 8 and 9). It is the photoselection effect due to the polarized excitation light that allows us to distinguish LAURDAN in the different lipid environments at the top region of the vesicles. An important observation here is that lines span both monolayers of the lipid membrane (Fig. 8).

From the LAURDAN GP data, we found a broad GP histogram centered at −0.2 at 45°C (Fig. 9). Below 36°C, at the phase coexistence region, the GP histogram is broader compared to that obtained in the fluid phase. The GP distribution of a single GUV at 28°C fits well to a bimodal histogram with centers at 0.10 and 0.29. The width of the LAURDAN GP histogram centered at 0.10 is larger than the width of the GP histogram centered at 0.29.

DISCUSSION

GUVs formed by DPPE/DPPC mixtures

Table 1 shows a comparison among our data and results from the literature for the DPPE/DPPC 7:3 and 3:7 (mol/mol) mixtures. As pointed out by Blume et al., a good agreement is found in the liquidus curve of the phase diagram of the DPPE/DPPC mixture by the use of different techniques (Blume et al., 1982). However, the temperature for the melting onset for this mixture is still a matter of controversy. We found a close agreement between our data and those of Arnold et al. (see Table 1; Arnold et al., 1981). Except for the solid-fluid→solid temperature transition, we also obtained relatively good agreement with the data of Blume et al. (1982). The discrepancies shown in Table 1 probably arise from inherent differences between the methods of sample preparation. The advantage of our method resides in the fact that we can *directly* observe the process of phase separation in a single vesicle. Based on our GP and *N*-Rh-DPPE intensity images, we concluded that this sample presents a nonideal mixture, showing solid-solid immiscibility. This conclusion is supported by the *N*-Rh-DPPE intensity images obtained at temperatures below 42°C (Fig. 6). One of the main conclusions in the work of Arnold et al. is that there is no cocrystallization of DPPC and DPPE on cooling (Arnold et al., 1981). Our results confirm this conclusion. Between 58°C and 42°C in GUVs composed of DPPE/DPPC 7:3 (mol/mol) mixture, the LAURDAN GP images and histograms clearly show gel-liquid crystalline phase separation. The solid and fluid phases at the phase coexistence temperature region have a GP histogram similar to those found in the solid and fluid temperature regions of the same mixture. Moreover, the GP histograms for the solid and fluid regions at the phase coexistence temperature region are in close agreement with those reported for GUVs formed by pure phospholipid DTPC, DMPC, or DPPC) in the pure gel and pure liquid crystalline phases, respectively (Bagatolli and Gratton, 1999). The same behavior was observed for the DPPE/DPPC 3:7 mixture at temperatures corresponding to the phase coexistence (data not shown).

A cluster-like organization of a similar lipid mixture consisting of dimyristoylphosphatidylethanolamine/dimyristoylphosphocholine (DMPE/DMPC) had been found with electron microscopy (Sackmann, 1978; Sackmann and Feder, 1995). The diameter of the clusters was estimated to vary between 50 and 100 nm (Sackmann, 1978). We observed DPPE gel domains with sizes on the order of several microns (almost the diameter of the GUVs). We also found some similarities in the shape and size of the DPPE gel domains in our images and those obtained in pure DPPE monolayers at the phase transition region (Grainger et al., 1990). These authors found that the DPPE liquid condensed domains have a size of several microns (up to 50 μm), with

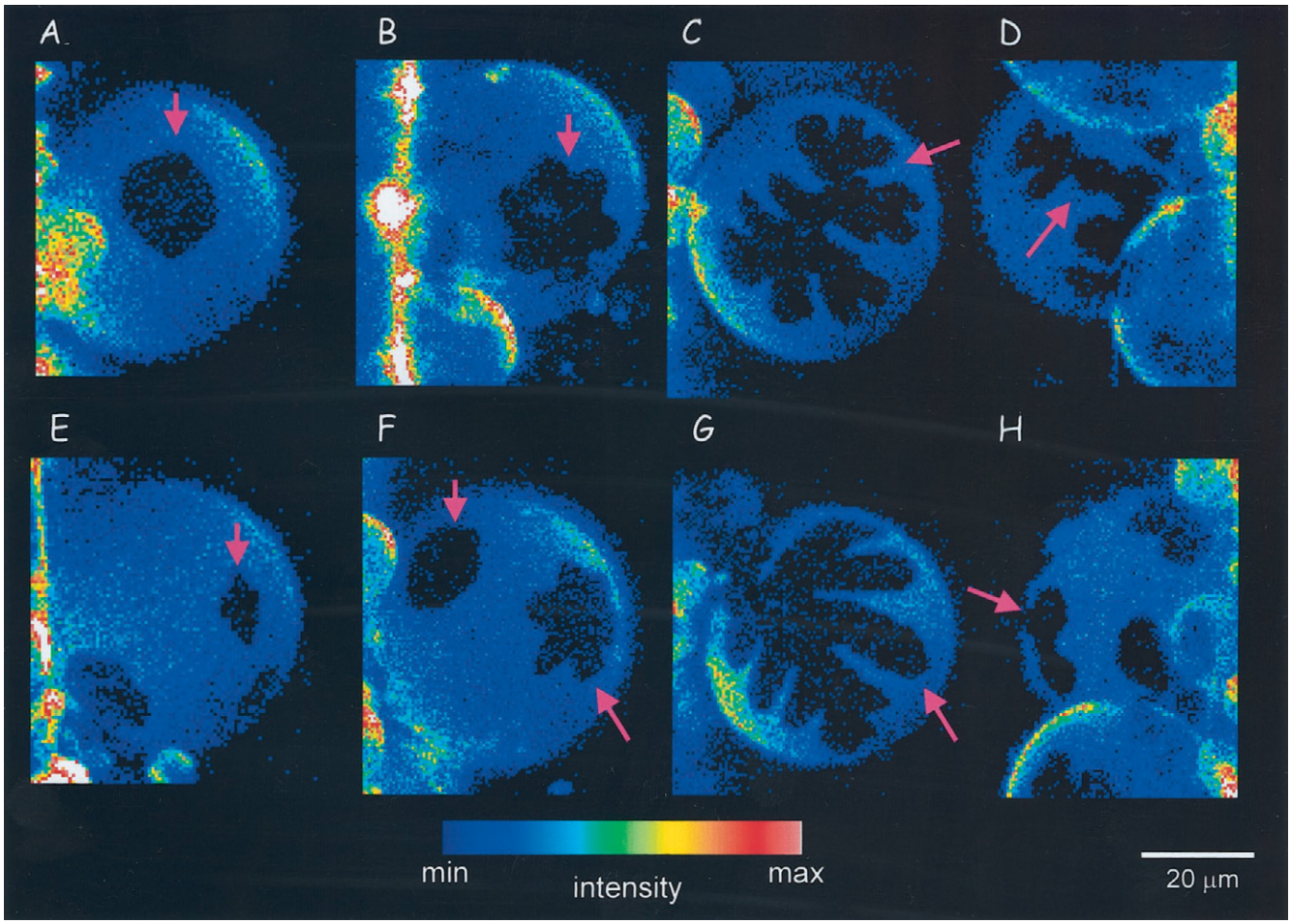

FIGURE 5 Different DPPE gel domain shapes in GUVs formed by DPPE/DPPC 7:3 and 3:7 (mol/mol) mixtures. The vesicles were labeled with *N*-Rh-DPPE. The two-photon excitation fluorescence intensity images were taken at the top of the GUV. The temperatures correspond to the phase coexistence region. (*A, B,* and *F*) DPPE/DPPC 3:7 (mol/mol) at 47.0, 46.4, and 46.0°C, respectively. (*C, D, E, G,* and *H*) DPPE/DPPC 7:3 (mol/mol) at 53.3, 55.0, 58.0, 48.0, and 56°C, respectively. The pink arrows indicate the different domain shapes. The images show fluorescence intensity in false color representation.

a dendritic appearance similar to that we observed for the DPPE gel domains in GUVs formed by the DPPE/DPPC mixture. The similarities between the shape and size of the liquid condensed DPPE domains in monolayers and the gel DPPE domains found in DPPE/DPPC GUVs provide an important point of comparison between these two systems. Based on these observations, we believe that the size of the DPPE gel domains is dependent on the curvature of the lipid vesicle.

Phase separation in vesicles composed of lipid mixtures produces a wide variety of shapes (Sackmann and Feder, 1995). Sackmann and Feder describe this process in terms of a combination of the theory of spinoidal decomposition and the membrane bending energy concept (Sackmann and Feder, 1995). These authors show different domain shapes obtained by electron microscopy as stripe-like arrangements of two-dimensional precipitates and hexagonal arrangements of circular domains, both predicted by the theory. They also mention that plane-wave domains have been obtained in membranes exhibiting gel-fluid coexistence, whereas circular domains are commonly observed in cases of fluid-fluid demixing (Sackmann and Feder, 1995). In our experiments, we observed a high diversity of domain shapes at temperatures corresponding to the phase coexistence in the DPPE/DPPC mixture as hexagonal, rhombic, six-cornered star, dumbbell, and dendritic shape. We also observed the dendritic shape and some quasicircular domains in the solid region of this mixture. This experimental information will be useful for future theoretical models. Our experimental approach greatly improves the capability to observe vesicles without any additional treatment, such as the staining process in the electron microscopy technique, which has been used very often to observe domain shapes in lipid mixtures.

One of the most interesting observations concerns the symmetry of DPPE's gel domains along the normal to the

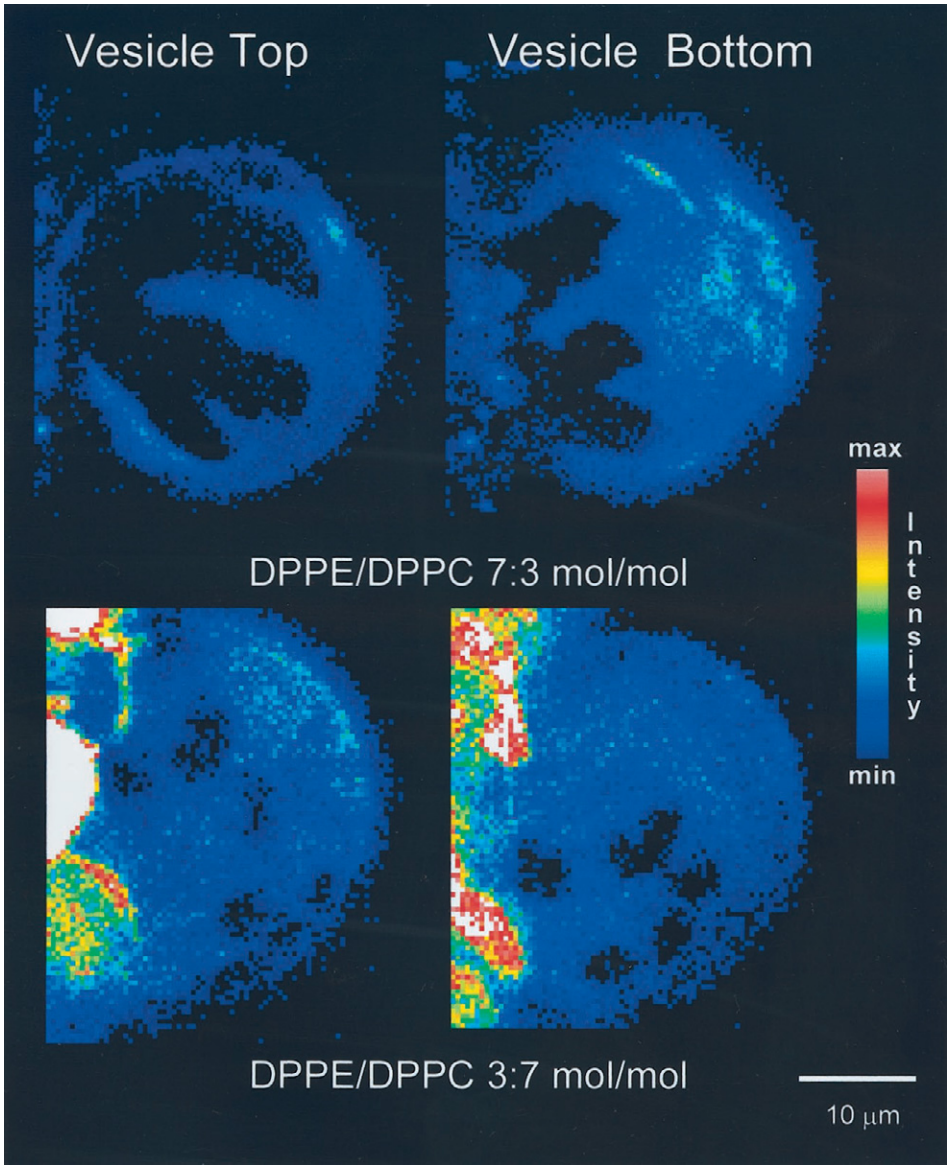

FIGURE 6 DPPE and DPPC gel domain in GUVs formed by DPPE/DPPC 7:3 and 3:7 (mol/mol) mixtures. The vesicles were labels with *N*-Rh-DPPE. The two-photon excitation fluorescence intensity images have been taken at the top and the bottom part of the GUV. The temperatures was 38°C. The images show fluorescence intensity in false color representation.

bilayer surface. This result shows a coupling between the inner and outer leaflets of the bilayer. DPPE can participate in intermolecular hydrogen bonding (Boggs, 1987). This intermolecular hydrogen bonding capability is one of the main reasons for the difference in the phase transition temperature between vesicles composed of pure DPPE and those composed of pure DPPC. These glycerol-based lipids have different polar headgroups and the same hydrophobic moiety. This particular characteristic (the intermolecular hydrogen bond capability of DPPE) can only explain the separation in one leaflet of the bilayer. While a model of the outer monolayer–inner monolayer coupling is beyond the scope of this article, we want to point out that it could be possible that the different molecular arrangement of the lipid molecules in the gel phase enhances the phospholipid tail-tail interaction. These tail-tail interactions could drive the formation of a lipid cluster from one side of the bilayer plane to the other.

GUVs formed by DLPC/DPPC mixtures

In this mixture we observed a strong influence of one phase on the other at temperatures corresponding to the fluid-solid phase coexistence. From the LAURDAN GP images and histograms we can conclude that the GP values in coexisting phases in this mixture are different from the GP of the pure gel phase coexisting with a pure liquid crystalline phase. This observation is in agreement with previous studies on multilamellar vesicles composed of DLPC/DPPC mixtures, based on LAURDAN′s GP and time-resolved emission spectra data (Parasassi et al., 1993). Based on LAURDAN′s

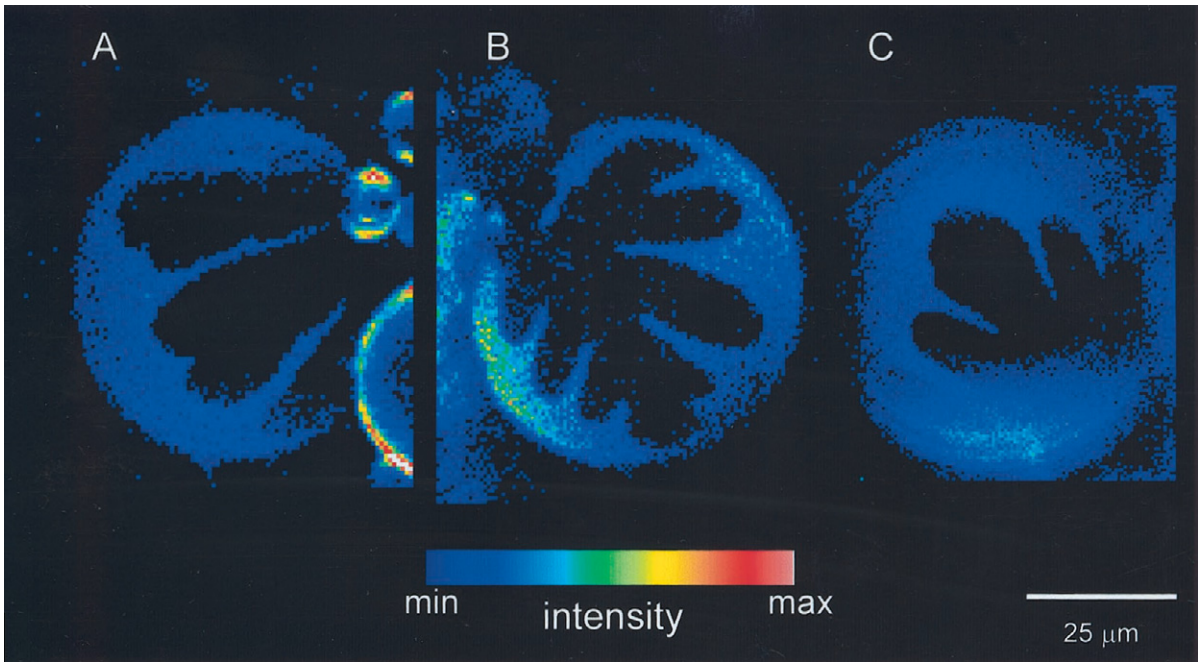

FIGURE 7 Two-photon excitation fluorescence intensity images (false color representation) of GUVs formed by DPPE/DPPC 7:3 mol/mol labeled with PRODAN (*A*), *N*-Rh-DPPE (*B*), and LAURDAN (*C*) at 53.0°C. The images have been taken at the top part of the GUV.

fluorescence behavior in vesicles composed of DLPC/DPPC mixtures, Parasassi et al. proposed two models to explain their results. The first model assumes that instead of forming a homogeneous phase, a small amount of DPPC in DLPC forms a phase that has a particular topology and does not display the properties of the pure gel phase. This phase can be represented as filaments of a gel into a liquid crystalline phase (Parasassi et al., 1993). The second model assumes fast interconversion between phases and very small size domains, on the order of 20–50 Å (Parasassi et al., 1993). We can conclude that the first model proposed by Parasassi et al. is in agreement with the microscopic picture found in our intensity images. From the PRODAN and LAURDAN intensity images and GP values we conclude that the lines we observed on the GUV surface at temperatures corresponding to the phase coexistence are composed mainly of DPPC but contain a fraction of DLPC. Decreasing the temperature increases the thickness of these gel-like line domains. From our pictures we observed that these lines (in the plane of the membranes) are several microns long (up to 30 μm) and on the order of several microns thick (up to 5 μm at low temperatures). Moreover, the lines move. The fluid→solid-fluid transition temperature for the DLPC/DPPC 1:1 mixture was 36°C in our experiments. Our temperature fluid→solid-fluid transition temperature is higher than that obtained from the phase diagram reported by Van Dijck et al. (~30°C) (Van Dijck et al., 1977). Unfortunately, we were not able to obtain the picture of the solid state for this mixture for technical reasons (DLPC has a transition temperature below 0°C).

Our observations are in contrast with those of Gliss et al. for mixtures of synthetic lecithins with a difference in chain length of four methylene groups (Gliss et al., 1998). These authors studied oriented lipid multilayers and supported lipid bilayers by grazing incidence neutron diffraction and atomic force microscopy, respectively. One of the main conclusions of their work is that the gel lipid domains at the phase coexistence region present irregular shapes with an average size of 10 nm (Gliss et al., 1998). Also for the coexistence region they suggest that domains grow in number rather than in size with decreasing temperature. We believe that the differences between our results and those obtained by Gliss et al. originate in the different physical characteristic of the samples. It is possible that the vesicle radius of curvature is an important parameter that influences the size and shape of lipid domains.

In multilamellar vesicles composed of DOPC/DPPC 1:1 (mol/mol) mixtures, Parasassi et al. showed, using two-photon excitation microscopy, that the size of the domains at the phase coexisting region is smaller than the pixel size (~200 μm) (Parasassi et al., 1997). We believe that in multilamellar vesicles the line-shaped domains may be very difficult to directly visualize by microscopy. In the case of a multilamellar vesicle the total fluorescence signal per pixel is an average of the fluorescence contribution of several bilayers, and the size of the pixel includes the dimension perpendicular to the membrane surface.

From the LAURDAN intensity pictures taken at the top of the vesicle we observed that the line-shaped domains present symmetry along the normal to the bilayer surface.

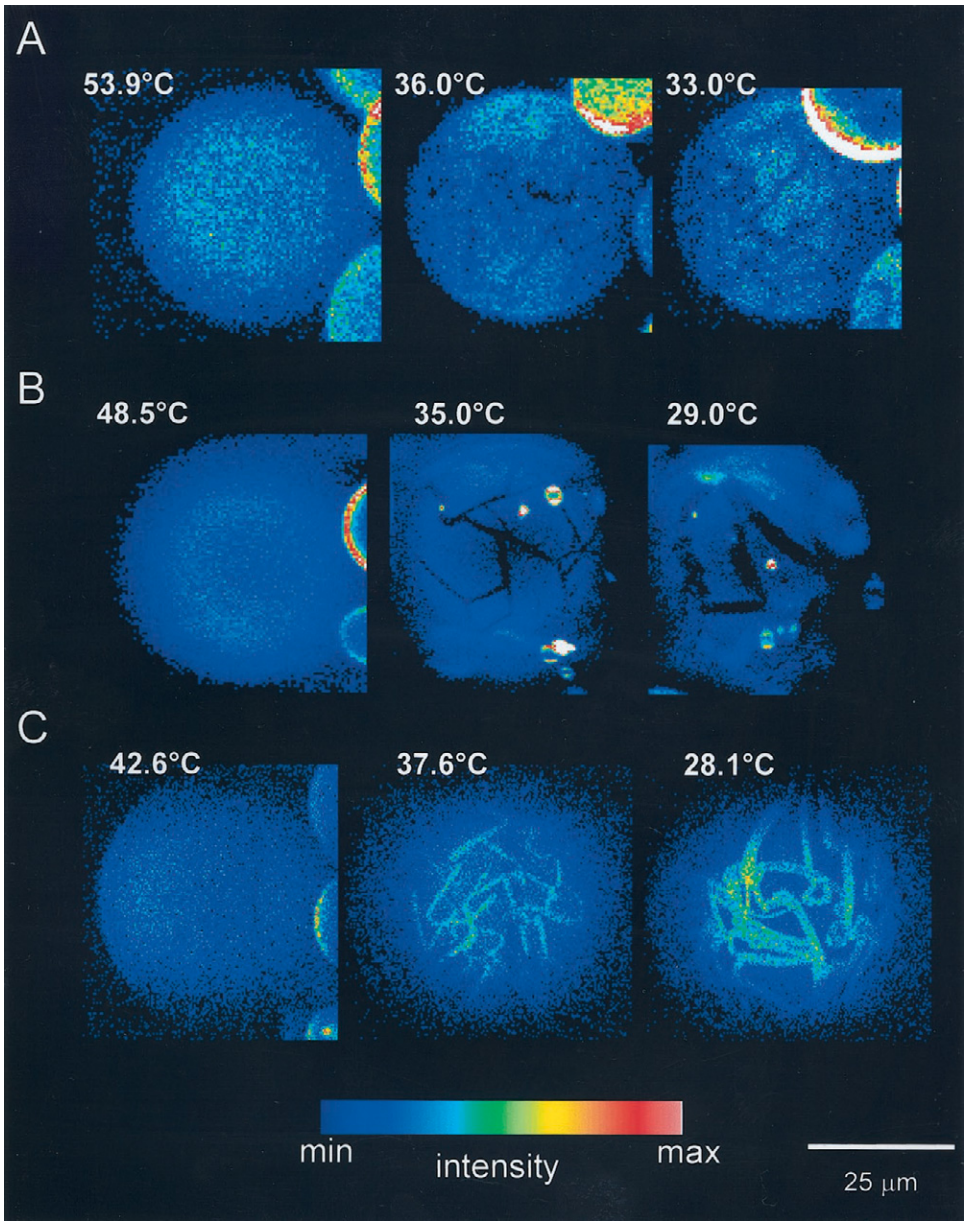

FIGURE 8 Two-photon excitation fluorescence intensity images (false color representation) of GUVs formed by DLPC/DPPC 1:1 (mol/mol) labeled with PRODAN (*A*), LAURDAN (*B*), and *N*-Rh-DPPE (*C*). The images have been taken at the top part of the GUV.

This picture is in agreement with that observed for GUVs composed of DPPE/DPPC mixtures. For instance, we propose that the mechanism that drives the domain symmetry normal to the bilayer surface can be generalized for phospholipid mixtures at the phase coexisting temperature region.

The observation of line-shaped domains in the DLPC/DPPC 1:1 (mol/mol) mixture is in agreement with previous observations made in GUVs composed of pure phospholipids (Bagatolli and Gratton, 1999). We reported that during the heating cycle the GUVs composed of pure DMPC, DTPC, or DPPC show a polygonal shape at the phase transition temperature. The proposed microscopic picture of the GUV polygonal shape was explained, assuming that the gel phase regions of the lipid bilayer become planar and that the vesicle bends along fluid line defects formed by liquid crystalline domains (Bagatolli and Gratton, 1999).

Comparison between GUVs composed of DPPE/DPPC and DLPC/DPPC mixtures

We can compare these different phospholipid mixtures in the fluid state and in the phase coexistence region. For both mixtures the fluid state is homogeneous in terms of the PRODAN, LAURDAN, and *N*-Rh-DPPE fluorescence intensity images. However, using the LAURDAN GP images, we found broad GP histograms in the fluid phase of the phospholipid mixtures. This observation is in line with previous observations made in GUVs composed of pure

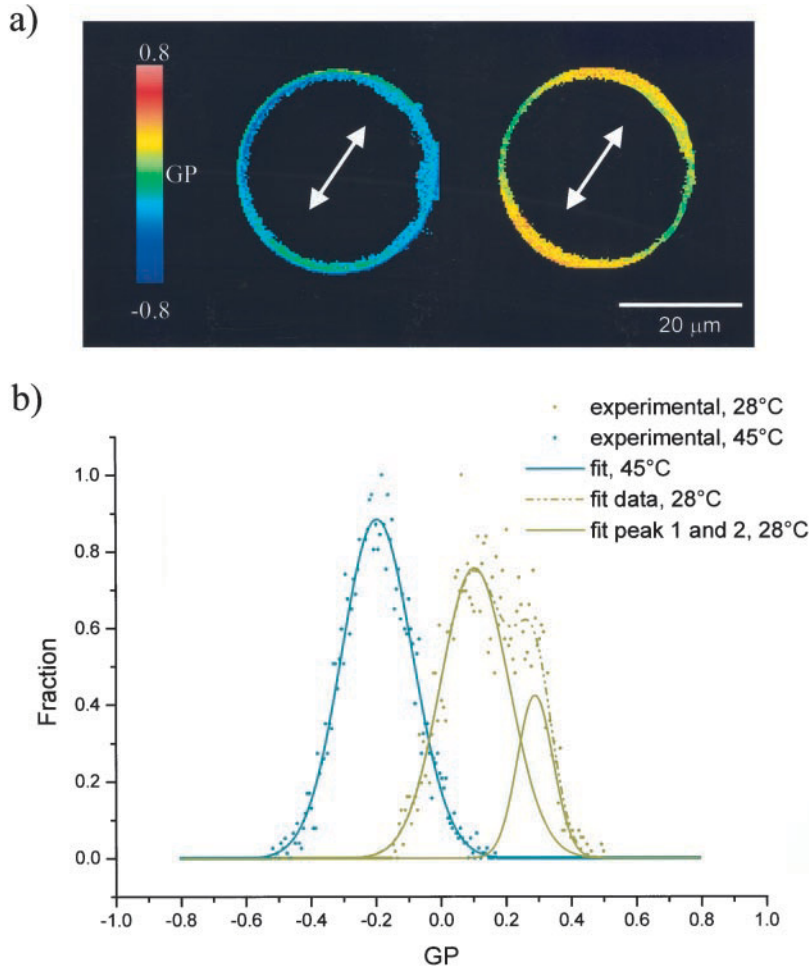

FIGURE 9 (*a*) Two-photon excitation LAURDAN GP images of a single GUV composed of DLPC/DPPC (1:1) obtained with polarized light in the fluid phase (*left*) and in the fluid-solid phase coexistence region (*right*). (*b*) Experimental and fitted GP histograms corresponding to the images presented in *a*. For the fitting procedure we used Gaussian functions.

DLPC, POPC, DTPC, DMPC, or DPPC and multilamellar vesicles composed of DOPC or DLPC (Bagatolli and Gratton, 1999; Parasassi et al., 1997). LAURDAN is sensitive to the water content in phospholipid interfaces (Parasassi and Gratton, 1995; Parasassi et al., 1998). To explain the heterogeneity in the LAURDAN GP histogram obtained in the liquid crystalline phase of DOPC and DLPC multilamellar vesicles, Parasassi et al. proposed the following model. In the liquid crystalline phase there is a distribution of sites with different sizes in which the LAURDAN molecule can reside (Parasassi et al., 1997). The larger the number of water molecules in the site the lower the GP value and the larger the cavity around the LAURDAN molecule (Parasassi et al., 1997). In the work by Parasassi et al., the authors also concluded that the domain size in the liquid crystalline phase was smaller than the microscope resolution (~200 nm). This conclusion was recently extended to the liquid crystalline phase of GUVs composed of pure POPC, DLPC, DTPC, DMPC, and DPPC (Bagatolli and Gratton, 1999). From our results for GUVs composed of DPPE/DPPC and DLPC/DPPC mixtures we conclude that the domain size in the fluid region is smaller than the microscope resolution, in agreement with previous observations (Parasassi et al., 1997; Bagatolli and Gratton, 1999).

At the phase coexistence region, the different nature of the phospholipid mixtures was clearly observed in our experiments. In the case of GUVs composed of DPPE/DPPC mixture, the different coexisting domains have pure liquid crystalline and pure gel phase characteristics. In contrast, in GUVs composed of the DLPC/DPPC 1:1 (mol/mol) mixture a strong influence on one phase by another was observed, i.e., gel-like phase coexisting with the liquid crystalline phase. Our approach, namely combining the LAURDAN GP images with the direct observation of the GUV surface, allows us for the first time to compare the topologies of different lipid mixtures. Furthermore, we can now pose new questions about these systems. Are the line-like domains a general picture for the mixtures of different chain length phosphatidylcholine phospholipids? Can we observe the same vesicle's lateral organization pattern obtained in GUVs composed of DPPE/DPPC mixtures in other samples that display pure gel–pure liquid crystalline phase separation? At present we lack the experimental evidence to generalize our observations. However, the similar pictures

TABLE 1 Comparison among the fluid and the solid-fluid → solid transition temperatures for DPPE/DPPC 7:3 and 3:7 (mol/mol) mixtures obtained by different techniques

X_{DPPE}	Fluid → solid-fluid (°C)	Solid-fluid → solid (°C)	Sample	Technique
0.7	58	42	GUVs	Two-photon excitation mycroscopy*
0.3	49	42		
0.7	59	43	MLVs	^{31}P NMR†
0.3	51	42		
0.7	60	46	MLVs	^{13}C and ^{2}H NMR‡
0.3	50	42		
0.7	58	54	MLVs	ESR and computer simulation§
0.3	50	45		
0.7	60	55	MLVs	Temperature gradient method using time-resolved x-ray difraction¶
0.3	52	46		

*This work.
†Arnold et al. (1981).
‡Blume et al. (1982).
§Ipsen and Mouritsen (1988).
¶Caffrey and Hing (1987).

obtained between GUVs formed by POPC/DPPC 1:1 (mol/mol) and DLPC/DPPC 1:1 (mol/mol) may help in principle to answer the first question.

A question may arise about the conditions used in preparing the GUVs. In general, the preparation of giant unilamellar vesicles requires no salt or very low salt concentration in the medium (Evans and Kwok, 1982; Angelova et al., 1992). This fact could, in principle, affect some physical properties of the membrane compared with the usual medium for bilayer studies (dilute salt concentrations). However, the good correlation between our data and some phase diagrams reported in the literature (in particular the liquidus curve) and the very good agreement between the LAURDAN GP values obtained in fluorescence cuvette analysis in the presence of salts and those obtained in the GUVs (Bagatolli and Gratton, 1999) suggest that this effect, if present, does not influence the lipid phases. Furthermore, we want to state that the GUV images obtained using three different fluorescent probes at the phase coexistence region (see Figs. 7 and 8) clearly show similar domain shapes for a particular mixture independently of the chemical structure of the fluorescent probe. Therefore, we rule out the possibility that traces of these three completely different molecules, i.e., N-Rh-DPPE, LAURDAN, and PRODAN, may have affected the formation of the lipid membrane domains.

Two-photon excitation with polarized light provides detailed information about the location of the probe in the lipid bilayer.

We obtained from our data experimental evidence of the location of the electronic transition dipoles in the lipid bilayer for *N*-Rh-DPPE and PRODAN. Fig. 10 shows the effect of the polarization of the excitation light on images of GUVs composed of DLPC/DPPC 1:1 (mol/mol) labeling with *N*- Rh-DPPE, PRODAN, or LAURDAN. The orientation of the excitation light polarization is shown in Fig. 10. The position of LAURDAN′s electronic transition dipole was reported to be parallel to the normal of the lipid bilayer (Parasassi and Gratton, 1995; Parasassi et al., 1997, 1998; Bagatolli and Gratton, 1999). If we excite a plane that passes through the center of the vesicle, we can photoselect the LAURDAN dipoles that are parallel to the direction of the excitation light (Fig. 10; Parasassi et al., 1997; Bagatolli and Gratton, 1999). Using the same polarization direction of the excitation light, we observed that the more intense fluorescent areas in the vesicles labeled with *N*-Rh-DPPE are located perpendicular to the orientation of the polarization of the excitation light (Fig. 10). Our conclusion is that the electronic transition dipole of *N*-Rh-DPPE is oriented parallel to the plane of the bilayer. This conclusion is in agreement with previous observations made with 1,32-dihydroxy-dotriacontane-bis-rhodamine 101 ester and rhodamine octadecanyl ester in DOPC bilayers (Karolin et al., 1995). A sketch of the probe location is also presented in Fig. 10. PRODAN′s electronic transition dipole orientation in the lipid bilayer is similar to that found for LAURDAN. However, the degree of photoselection is less than that for LAURDAN. This may be because PRODAN, in contrast to LAURDAN, is located in the polar headgroup region of the lipid membrane close to bulk water (see Fig. 10; Chong and Wong, 1993; Krasnowska et al., 1998). This location should allow for a more heterogeneous distribution in the PRODAN′s orientation compared with LAURDAN, which is located deeper in the lipid membrane.

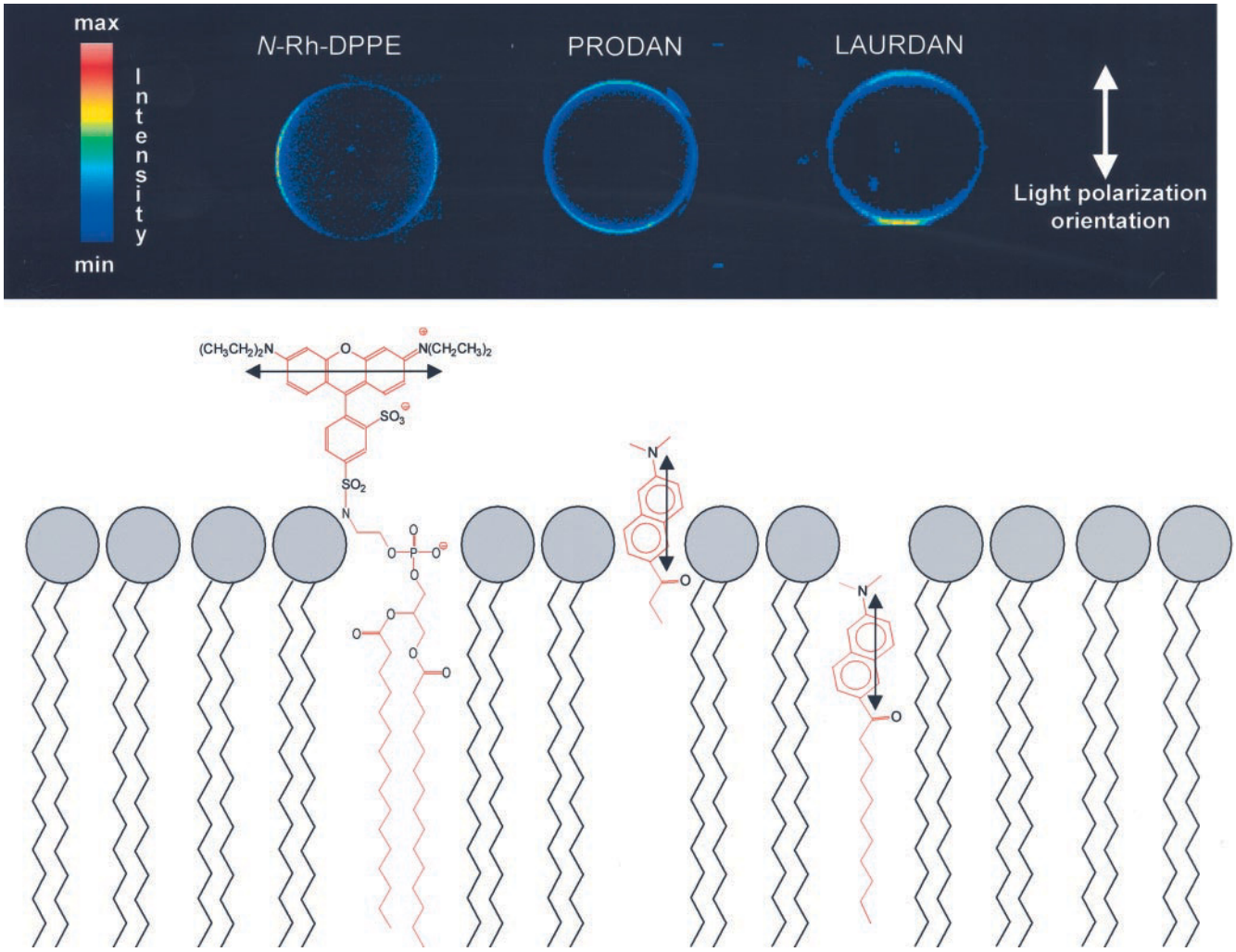

FIGURE 10 (*Top*) Two-photon excitation fluorescence intensity images (false color representation) of GUVs formed by DLPC/DPPC 1:1 (mol/mol) labeled with *N*- Rh-DPPE, PRODAN, and LAURDAN. The images have been taken at the center part of the GUV with polarized light. The temperature was 25°C. (*Bottom*) Sketch showing the location of the fluorescent molecules in the lipid membrane.

Another important observation, pointed out in the Results section, concerns the partition of these different probes in the different lipid phases. Our data demonstrated a homogeneous LAURDAN distribution in the region of phase coexistence in GUVs composed of DPPE/DPPC and DLPC/DPPC mixtures (see Fig. 2 and 9). However, the effect of photoselection due to the polarization of the excitation light allows discrimination between the rigid and fluid domains at the top or bottom of the lipid vesicles. The rigid domains obtained in the top or bottom regions in the LAURDAN-labeled GUVs are nonfluorescent.

A different picture is found in the PRODAN two-photon excitation intensity images. PRODAN′s partition is different between the different lipid phases. Krasnowska et al. pointed out that at 25°C the PRODAN partition coefficient from water to the lipid liquid crystalline phase is higher by a factor of ~35 with respect to that found in the gel phase (Krasnowska et al., 1998). A similar effect was observed by Zeng and Chong (1995). These observations are in agreement with our results on PRODAN-labeled GUVs formed by DPPE/DPPC and DLPC/DPPC mixtures. In the case of PRODAN-labeled GUVs composed of DLPC/DPPC 1:1 (mol/mol) mixture, we observed a considerably lower intensity coming from the gel-like line domains than from the fluid part of the vesicle. In contrast, in the DPPE/DPPC 7:3 (mol/mol) mixture the rigid domains are nonfluorescent. We speculate that in the case of DPPE gel domains the partition coefficient of PRODAN should be even lower than in the gel phase of phosphatidylcholine phospholipids. The very stable arrangement of the DPPE gel phase, mainly due to the intermolecular hydrogen-bonding network in the polar headgroup region of the membrane (Boggs, 1987), suggests that PRODAN needs extra energy to partition from the aqueous phase to the DPPE gel phase.

Finally, we want to discuss the case of *N*-Rh-DPPE. This fluorescent probe shows a total segregation from the DPPE

gel domains in GUVs formed by DPPE/DPPC mixtures. The *N*-Rh-DPPE molecule has a very large polar headgroup due to the rhodamine moiety and cannot easily be inserted into the DPPE gel phase. Therefore the *N*-Rh-DPPE molecules are segregated to the fluid domains. In the case of DLPC/DPPC mixtures the situation is different. The intensity coming from the gel-like line domains is higher than that coming from the fluid parts. To explain this phenomenon we consider: 1) Absence of strong polar headgroup interactions among the DPPC molecules compared with those found among DPPE molecules in the gel phase (this observation is consistent with the picture observed in GUVs formed by DPPE/DPPC in the solid region. In this case the fluorescence comes from the DPPC gel domains). 2) The favorable interaction of the hydrophobic moieties of *N*-Rh-DPPE and DPPC molecules (the hydrophobic moieties of *N*-Rh-DPPE and DPPC molecules match, while the DLPC hydrophobic moiety is shorter than DPPC). 3) Our observation of gel-like domains coexisting with fluid domains in the DLPC/DPPC mixture can explain the particular *N*-Rh-DPPE partition. In this case the DLPC molecules that cocrystallize with the DPPC molecules can create defects allowing a favorable partition of *N*-Rh-DPPE molecules in the gel-like phase. We note that the presence of *N*-Rh-DPPE dimers, i.e., nonfluorescent rhodamine complexes, is unlikely at the low probe concentration utilized in the experiments.

CONCLUSION

A novel microscopic picture of two-component lipid membranes is presented in this work. With our experimental approach, we have the advantage of correlating lipid phase behavior with the lateral topology of the GUVs. The direct observation of lipid domain characteristics such as size, shape, and dynamics in GUVs composed of phospholipid mixtures having different polar headgroups but equal hydrophobic chain length size or equal polar headgroups but different hydrophobic chain length size offers *direct* experimental evidence of the temperature behavior of these lipid samples. The combination of the two-photon excitation images, the polarization of the excitation light, and the fluorescent and partition properties of LAURDAN, PRODAN, and *N*-Rh-DPPE molecules in the different lipid phases offer a unique advantage in the study of phase coexistence in different lipid mixtures.

We thank Dr. J. D. Müller for the help with the chamber design and for the chamber construction and Dr. D. M. Jameson for critical reading of the manuscript.

This work was supported by the National Institutes of Health (RR03155). LAB is a recipient of a CONICET (Argentina) fellowship.

REFERENCES

Angelova, M. I., and D. S. Dimitrov. 1986. Liposome electroformation. *Faraday Discuss. Chem. Soc.* 81:303–311.

Angelova, M. I., S. Soléau, Ph. Meléard, J. F. Faucon, and P. Bothorel. 1992. Preparation of giant vesicles by external AC fields. Kinetics and application. *Prog. Colloid Polym. Sci.* 89:127–131.

Arnold, K., A. Lösche, and K. Gawrisch. 1981. ^{31}P-NMR investigations of phase separation in phosphatidylcholine/phosphatidylethanolamine mixtures. *Biochim. Biophys. Acta.* 645:143–148.

Bagatolli, L. A., and E. Gratton. 1999. Two-photon fluorescence microscopy observation of shape changes at the phase transition in phospholipid's giant unilamellar vesicles. *Biophys. J.* 77:2090–2101.

Bagatolli, L. A., E. Gratton, and G. D. Fidelio. 1998. Water dynamics in glycosphingolipids studied by LAURDAN fluorescence. *Biophys. J.* 75:331–341.

Bagatolli, L. A., B. Maggio, F. Aguilar, C. P. Sotomayor, and G. D. Fidelio. 1997. LAURDAN properties in glycosphingolipid-phospholipid mixtures: a comparative fluorescence and calorimetric study. *Biochim. Biophys. Acta.* 1325:80–90.

Blume, A., R. J. Wittebort, S. K. Das Gupta, and R. G. Griffin. 1982. Phase equilibria, molecular conformation, and dynamics in phosphatidylcholine/phosphatidylethanolamine bilayers. *Biochemistry.* 21:6243–6253.

Boggs, J. M. 1987. Lipid intermolecular hydrogen bonding: influence on structural organization and membrane function. *Biochim. Biophys. Acta.* 906:353–404.

Caffrey, M., and F. S. Hing. 1987. A temperature gradient method for lipid phase diagram construction using time-resolved x-ray diffraction. *Biophys. J.* 51:37–46.

Chong, P. L. G., and P. T. T. Wong. 1993. Interactions of Laurdan with phosphatidylcholine liposomes: a high pressure FTIR study. *Biochim. Biophys. Acta.* 1149:260–266.

Dimitrov, D. S., and M. J. Angelova. 1987. Lipid swelling and liposome formation on solid surfaces in external elctric fields. *Prog. Colloid Polym. Sci.* 73:48–56.

Evans, E., and R. Kwok. 1982. Mechanical calorimetry of large dimyristoylphosphatidylcholine vesicles in the phase transition region. *Biochemistry.* 21:4874–4879.

Gebhardt, C., H. Gruler, and E. Sackmann. 1977. On domain structure and local curvature in lipid bilayer and biological membranes. *Z. Naturforsch.* 32C:581–596.

Gliss, C., H. Clausen-Schaumann, R. Gunther, S. Odenbach, O. Randl, and T. M. Bayerl. 1998. Direct detection of domains in phospholipid bilayers by grazing incidence diffraction of neutrons and atomic force microscopy. *Biophys. J.* 74:2443–2450.

Grainger, D. W., A. Reichert, H. Ringsdorf, and C. Salesse. 1990. Hydrolitic action of phospholipase A2 in monolayers in the phase transition region: direct observation of enzyme domain formation using fluorescence microscopy. *Biochim. Biophys. Acta.* 1023:365–379.

Hauser, H., and G. Poupart. 1992. Lipid structure. *In* The Structure of Biological Membranes. P. Yagle, editor. CRC Press, Boca Raton, Ann Arbor, and London. 34–37.

Ipsen, J. H., and O. G. Mouritsen. 1988. Modelling the phase equilibria in two-components membranes of phospholipids with different acyl-chain lengths. *Biochim. Biophys. Acta.* 944:121–134.

Jørgensen, K., and O. G. Mouritsen. 1995. Phase separation dynamics and lateral organization of two-component lipid membranes. *Biophys. J.* 69:942–954.

Karolin, J., S. Bogen, L. B. Johansson, and J. G. Molotkovsky. 1995. Polarized fluorescence and absorption spectroscopy of 1,32-dihydroxydotriacontane-*bis*-rhodamine 101 ester. A new and lipid bilayer-spanning probe. *J. Fluorescence.* 5:279–284.

Krasnowska, E., E. Gratton, and T. Parasassi. 1998. Prodan as a membrane surface fluorescence probe: partitioning between water and phospholipid phases. *Biophys. J.* 74:1984–1993.

Lasic, D. D. 1988. The mechanism of vesicle formation. *Biochem. J.* 256:1–11.

Lee, A. G. 1975. Fluorescence studies of chlorophyll a incorporated into lipid mixtures and the interpretation of "phase" diagrams. *Biochim. Biophys. Acta.* 413:11–23.

Lentz, B. R., Y. Barenholtz, and T. E. Thompson. 1976. Fluorescence depolarization studies of phase transitions and fluidity in phospholipid bilayers. 2. Two-component phosphatidylcholine liposomes. *Biochemistry.* 15:4529–4537.

Mabrey, S., and J. M. Sturtevant. 1976. Investigation of phase transition of lipids and lipid mixtures by high sensitivity differential scanning calorimetry. *Proc. Natl. Acad. Sci. USA.* 73:3862–3866.

Mathivet, L., S. Cribier, and P. F. Devaux. 1996. Shape change and physical properties of giant phospholipid vesicles prepared in the presence of an AC electric field. *Biophys. J.* 70:1112–1121.

Meléard, P., C. Gerbeaud, P. Bardusco, N. Jeandine, M. D. Mitov, and L. Fernandez-Puente. 1998. Mechanical properties of model membranes studied from shape transformations of giant vesicles. *Biochimie.* 80: 401–413.

Meléard, P., C. Gerbeaud, T. Pott, L. Fernandez-Puente, I. Bivas, M. D. Mitov, J. Dufourcq, and P. Bothorel. 1997. Bending elasticities of model membranes: influences of temperature and sterol content. *Biophys. J.* 72:2616–2629.

Menger, F. M., and J. S. Keiper. 1998. Chemistry and physics of giant vesicles as biomembrane models. *Curr. Opin. Chem. Biol.* 2:726–732.

Needham, D., and E. Evans. 1988. Structure and mechanical properties of giant lipid (DMPC) vesicles bilayers from 20°C below to 10°C above the liquid crystal-crystalline phase transition at 24°C. *Biochemistry.* 27: 8261–8269.

Needham, D., T. M. McIntosh, and E. Evans. 1988. Thermomechanical and transition properties of dimyristoylphosphatidylcholine/cholesterol bilayers. *Biochemistry.* 27:4668–4673.

Parasassi, T., G. De Stasio, A. d'Ubaldo, and E. Gratton. 1990. Phase fluctuation in phospholipid membranes revealed by LAURDAN fluorescence. *Biophys. J.* 57:1179–1186.

Parasassi, T., G. De Stasio, G. Ravagnan, R. M. Rusch, and E. Gratton. 1991. Quantitation of lipid phases in phospholipid vesicles by the generalized polarization of LAURDAN fluorescence. *Biophys. J.* 60: 179–189.

Parasassi, T., and E. Gratton. 1995. Membrane lipid domains and dynamics detected by LAURDAN. *J. Fluorescence.* 5:59–70.

Parasassi, T., E. Gratton, W. Yu, P. Wilson., and M. Levi. 1997. Two photon fluorescence microscopy of LAURDAN generalized polarization domains in model and natural membranes. *Biophys. J.* 72:2413–2429.

Parasassi, T., E. Krasnowska, L. A. Bagatolli, and E. Gratton. 1998. LAURDAN and PRODAN as polarity-sensitive fluorescent membrane probes. *J. Fluorescence*. 8:365–373.

Parasassi, T., G. Ravagnan, R. M. Rusch, and E. Gratton. 1993. Modulation and dynamics of phase properties in phospholipid mixtures detected by LAURDAN fluorescence. *Photochem. Photobiol.* 57:403–410.

Sackmann, E. 1978. Dynamic molecular organization in vesicles and membranes. *Ber. Bunsenges. Phys. Chem.* 82:891–909.

Sackmann, E. 1994. Membrane bending energy concept of vesicle- and cell-shapes and shape-transitions. *FEBS Lett.* 346:3–16.

Sackmann, E., and T. Feder. 1995. Budding, fission and domain formation in mixed lipid vesicles induced by lateral phase separation and macromolecular condensation. *Mol. Membr. Biol.* 12:21–28.

Shimshick, E. J., and H. M. McConnell. 1973. Lateral phase separation in phospholipid membranes. *Biochemistry.* 12:2351–2360

So, P. T. C., T. French, W. M. Yu, K. M. Berland, C. Y. Dong, and E. Gratton. 1995. Time resolved fluorescence microscopy using two-photon excitation. *Bioimaging.* 3:49–63.

So, P. T. C., T. French, W. M. Yu, K. M. Berland, C. Y. Dong, and E. Gratton. 1996. Two-photon fluorescence microscopy: time-resolved and intensity imaging in fluorescence imaging spectroscopy and microscopy. X. F. Wang and B. Herman, editors. Chemical Analysis Series, Vol. 137. John Wiley and Sons, New York. 351–374.

Van Dijck, P. W. M., A. J. Kaper, H. A. J. Oonk, and J. De Gier. 1977. Miscibility properties of binary phosphatidylcholine mixtures. A calorimetric study. *Biochim. Biophys. Acta.* 470:58–69.

Yu, W., P. T. So, T. French, and E. Gratton. 1996. Fluorescence generalized polarization of cell membranes: a two-photon scanning microscopy approach. *Biophys. J.* 70:626–636.

Zeng, J., and P. L. Chong. 1995. Effect of ethanol-induced lipid interdigitation on the membrane solubility of Prodan, Acdan and Laurdan. *Biophys. J.* 68:567–573.